S_N2 and S_N2' reaction dynamics of cyclopropenyl chloride with halide ion — A direct ab initio molecular dynamics (MD) study[1]

Hiroto Tachikawa

Abstract: Direct ab initio molecular dynamics (MD) calculations have been carried out for the reaction of cyclopropenyl chloride with halide ion (F^-) ($F^- + (CH)_3Cl \rightarrow F(CH)_3 + Cl^-$) in gas phase. Both S_N2 and S_N2' channels were found as product channels. These channels are strongly dependent on the collision angle of F^- to the target $(CH)_3Cl$ molecule. The collision at one of the carbon atoms of the C=C double bond leads to the S_N2' reaction channel; whereas the collision at the methylene carbon atom leads to the S_N2 reaction channel. The reactions proceed via a direct mechanism without long-lived complexes. The reaction mechanism is discussed on the basis of the theoretical results.

Key words: S_N2 reaction, direct ab initio molecular dynamics, halogen exchange, reaction mechanism.

Résumé : On a effectué des calculs de dynamique moléculaire ab initio directs pour la réaction en phase gazeuse du chlorure de cyclopropényle avec l'ion fluorure (F^-) ($F^- + (CH)_3Cl \rightarrow F(CH)_3 + Cl^-$). On a trouvé que les voies S_N2 et S_N2' peuvent toutes les deux conduire au produit. Ces voies dépendent fortement de l'angle de collision du F^- sur la molécule cible $(CH)_3Cl$. Une collision sur un des atomes de carbone de la double liaison C=C conduit à une voie S_N2' alors qu'une collision sur l'atome de carbone méthylène conduit à une voie S_N2. La réaction se produit par le biais d'un mécanisme direct sans complexes de longue vie. On discute du mécanisme réactionnel sur la base des résultats théoriques.

Mots clés : réaction S_N2, calculs de dynamique moléculaire ab initio directs, échange d'halogène, mécanisme réactionnel.

[Traduit par la Rédaction]

Introduction

Bimolecular nucleophilic substitution (S_N2) reactions have been the focus of extensive theoretical and experimental works in recent years because of their central importance and basic reaction in organic and bioorganic chemistries (1, 2). In particular, the reaction of halide ion (X^-) plays an important role in several organic reactions.

For the reaction dynamics of the halogen exchange S_N2 reaction of a type, $X^- + RY \rightarrow RX + Y^-$ (X, Y = F, Cl, or Br), where R is an alkyl group. Hase and his co-workers (3, 4) have done extensive investigations by means of the classical trajectory method with ab initio fitted analytical potential energy functions. Several characteristic features for the halogen exchange S_N2 reactions have been elucidated from their results. However, the reactions previously investigated are only in the case of methyl halide (R = CH_3). There is no dynamics study on a more complicated system. This is due to the fact that dimension, which should be included in the calculation, will greatly increase as the number of atoms in the reaction system is increased. Therefore, the procedure of the fitting becomes more difficult and more complicated in a larger system.

In the present study, we have investigated a S_N2 reaction of cyclopropenyl chloride with halide ion (F^-), i.e., R = $(CH)_3$,

$$[1] \qquad F^- + (CH)_3Cl \rightarrow F(CH)_3 + Cl^-$$

by means of the direct ab initio molecular dynamics (MD) method. In this method, we do not need a fitting procedure of PES to an analytical function. Therefore, it is suitable to investigate a complex S_N2 reaction using the direct ab initio trajectory method. In previous papers, we have carried out direct ab initio MD calculations for the S_N2 reactions, $F^-(H_2O)_n + CH_3Cl$ (n = 0–1) (5–9) and $OH^- + CH_3Cl \rightarrow CH_3OH + Cl^-$ (10). Mechanism, collision energy dependence, and branching ratios of the product channels were predicted from the calculations. Also, it was suggested that the direct ab initio MD method is a powerful tool for investigating the reaction dynamics for the reactions with large degrees of freedom.

Figure 1 shows an illustration of the reaction scheme of cyclopropenyl chloride with halide ion (F^-). Cyclopropenyl chloride ($(CH)_3Cl$) is constructed of a three-membered ring with one double bond and a chlorine atom is substituted in the methylene (CH_2) group. Therefore, the reactive collisions of X^- ion take place in a σ attack S_N2 site, a π attack S_N2' (anti) site, and a π attack S_N2' (syn) site. For the reaction of F^-, three reaction channels will be expected: S_N2, S_N2' (anti), and S_N2' (syn).

Received 14 April 2005. Published on the NRC Research Press Web site at http://canjchem.nrc.ca on 1 December 2005.

H. Tachikawa. Division of Materials Chemistry, Graduate School of Engineering, Hokkaido University, Sapporo 060-8628, Japan (e-mail: hiroto@eng.hokudai.ac.jp).

[1]This article is part of a Special Issue dedicated to organic reaction mechanisms.

 doi: 10.1139/V05-176

Fig. 1. Schematic illustration of the reaction of cyclopropenylchloride with F^- (F^- + $(CH)_3Cl$). Three reaction channels are possible for reactive collision.

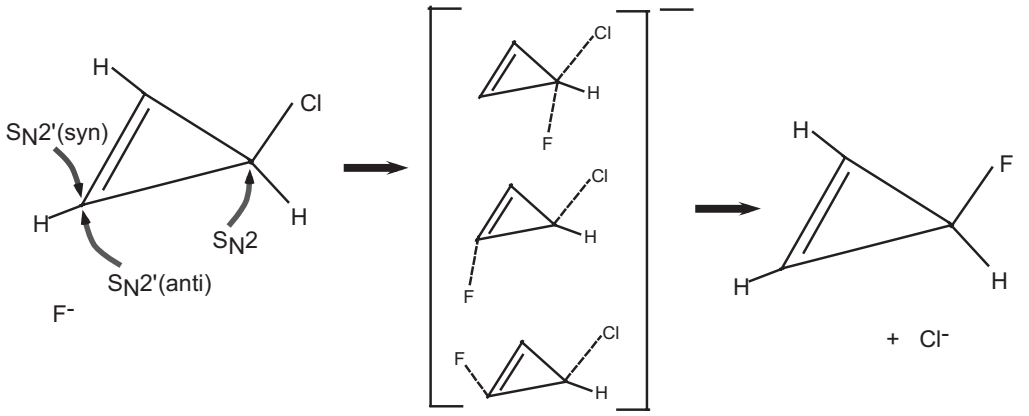

From a theoretical point of view, Kim et al. (11) investigated the potential energy diagram for the symmetric S_N2 reaction

[2] $X^- + (CH)_3X \rightarrow X(CH)_3 + X^-$ (X = F, Cl, or Br)

by means of ab initio calculation. Their calculations indicated that there are double minima corresponding to pre- and late-complexes, while the transition state is lower in energy than the initial separation. The barrier height increases in the order S_N2' (anti) < S_N2' (syn) < S_N2 for X = F. For the symmetric S_N2 rxn. [2], static ab initio calculations have been thus carried out (11), and the energetics are well-elucidated. On the other hand, there is no dynamics study for rxn. [1] because the reaction has many degrees of freedom ($3N - 6 = 18$, where N is the number of atoms in the reaction system). Furthermore, the energetics for the asymmetric reaction, $X^- + (CH)_3Y \rightarrow X(CH)_3 + Y^-$ (X or Y = F, Cl, or Br), are not clearly understood.

In the present paper, a direct ab initio MD calculation (12–15) is carried out for rxn. [1] to elucidate the reaction mechanism and to obtain the dynamics feature. The reaction mechanism will be discussed on the basis of theoretical results. Note that this work is the first study to investigate the dynamics of rxn. [1].

Methods of calculation

The Hartree–Fock (HF)/3-21+G(d) optimized geometry of $(CH)_3Cl$ was chosen as an initial structure. At the start of the trajectory calculation, atomic velocities of $(CH)_3Cl$ were adjusted to give a mean temperature of 10 K. Temperature of the reaction system is defined by

$$[3] \qquad T = \frac{1}{3kN}\left\langle \sum_i m_i v_i^2 \right\rangle$$

where N is number of atoms, v_i and m_i are the velocity and mass of the ith atom, and k is Boltzmann's constant.

Figure 2 shows the structure and geometrical parameters of the reaction system. We examined S_N2 and S_N2' (anti) collisions in the present work. At initial separations, i.e., F^- + $(CH)_3Cl$, the angles of F-$(CH)_3$-Cl (θ_1) were randomly generated from 0.0° to 180°. The distances between F^- and

Fig. 2. Geometrical parameters for the reaction system F^- + $(CH)_3Cl$.

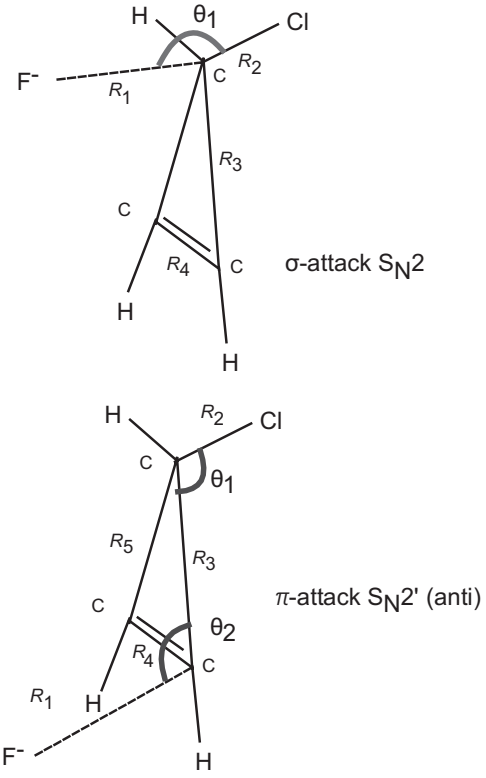

$(CH)_3Cl$ (R_1) were also generated within 8.0–10.0 Å. A total of 40 geometrical configurations were randomly generated, and 40 trajectories were analyzed for constant collision energy (E_{coll} = 5.0 kcal/mol, 1 cal = 4.184 J). The equations of motion for n atoms in the reaction system are given by

$$[4] \qquad \frac{dQ_j}{dt} = \frac{\partial H}{\partial P_j}$$
$$\frac{dP_j}{dt} = \frac{\partial H}{\partial Q_j} = \frac{\partial U}{\partial Q_j}$$

where j = 1–3N, H is the classical Hamiltonian, U is the potential energy of the reaction system, Q_j is the Cartesian co-

Fig. 3. Potential energy profile of the reaction $F^- + (CH)_3Cl \rightarrow (CH)_3F + Cl^-$, calculated at the B3LYP/6-311++G(d,p) and HF/3-21+G(d) levels. The values are relative energies (in kcal/mol) calculated at the B3LYP/6-311++G(d,p) level. The HF/3-21+G(d) values are given in parenthesis.

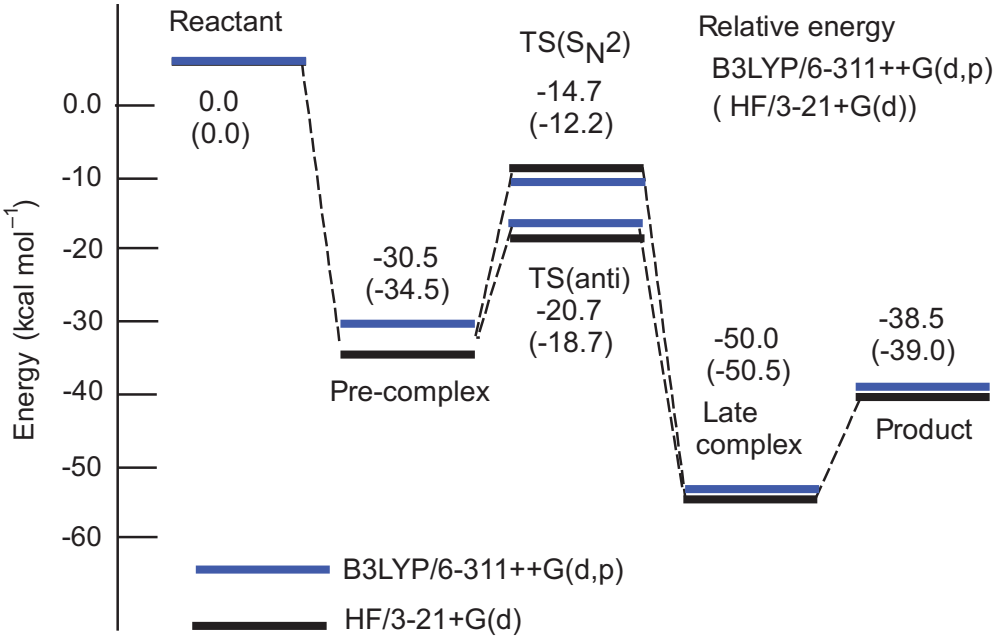

ordinate of the jth mode, and P_j is conjugated momentum. These equations were numerically solved by the standard fourth-order Runge–Kutta and sixth-order Adams–Moulton combined algorithm. No symmetry restriction was applied to the calculation of the gradients. The time step size was chosen as 0.2 fs, and a total of 5000 steps were integrated for each dynamics calculation. The drift of the total energy is confirmed to be less than 0.001% at all steps in the trajectory. The rotational quantum number of F^- at initial separation was assumed to be zero ($J = 0$). All static ab initio calculations were carried out using the GAUSSIAN03 program package (16).

Results and discussion

Potential energy diagram for the reaction

The potential energy diagram for rxn. [1] is illustrated in Fig. 3. The calculations are carried out at the B3LYP/6-311++G(d,p) level. The values obtained at the HF/3-21+G(d) level are also given for comparison. Zero level corresponds to the energy of the reactant at the initial separation between F^- and $(CH)_3Cl$. The precomplex, expressed by $F^-\cdots(CH)_3Cl$, was first formed in the entrance region. The binding energy of F^- to $(CH)_3Cl$ is calculated to be 30.5 kcal/mol at the B3LYP/6-311++G(d,p) level. From this point, the reaction is branched to two channels. These are the S_N2 and S_N2' (anti) channels. Both transition states (TS) for the two channels are lower in energy than that of the reactant. The energy levels of the TSs for S_N2 and S_N2' (anti) channels are calculated to be –14.7 and –20.7 kcal/mol relative to the reactant, respectively. These energy levels for S_N2 and S_N2' (anti) channels correspond to barrier heights of 15.8 and 9.8 kcal/mol relative to the precomplex, respectively.

After leaving the TS, the energy is suddenly decreased, and the reaction point reaches the late complex in the exit region. The late complex is expressed by $F(CH)_3\cdots Cl^-$, where one of the hydrogen atoms of $F(CH)_3$ orients the Cl^- ion. Finally, the reaction point reaches the product ($(CH)_3F + Cl^-$).

It should be noted that the energy diagram calculated at the HF/3-21+G(d) level resembles that of the B3LYP/6-311++G(d,p) level. The heat of reaction was calculated to be $-\Delta H = 39.0$ kcal/mol, which is in reasonable agreement with that of the higher level calculation (38.5 kcal mo1^{-1}). The energy levels for the TSs for S_N2 and S_N2' (anti) channels are –12.2 and –18.7 kcal/mol at the HF/3-21+G(d) level. The corresponding energies obtained were –14.7 and –20.7 kcal/mol at the B3LYP/6-311++G(d,p) level. Thus, the HF/3-21+G(d) calculation would give a reasonable multidimensional potential energy surface (PES) for the S_N2 reaction, $F^- + (CH)_3Cl \rightarrow F(CH)_3 + Cl^-$. At the very least, this level of theory is applicable to a qualitative argument for rxn. [1].

The relative energies for stationary points along the reaction $F^- + (CH)_3Cl$ are given in Table 1. Zero-point vibrational energies (ZPEs) are also considered in the relative energies (given in parenthesis). The relative energies for pre- and late-complexes and product state are similar to each other. It was found that the B3LYP calculation seems to slightly underestimate the barrier heights for rxn. [1] by comparison with the MP2 calculation.

The optimized structures at the stationary points of the $F^- + (CH)_3Cl$ reaction system are illustrated in Fig. 4. In the transition state for the S_N2 reaction channel denoted to TS(S_N2), the F^- ion is located at $R_1 = 2.360$ Å, while the C—Cl bond length is elongated to be $R_2 = 2.384$ Å. The angle for F-C-Cl was calculated to be 170°, implying that the structure at the transition state is close to collinear. The C—F and C—Cl bond lengths the transition state for the S_N2

Table 1. Relative energies (in kcal/mol) for stationary points along the reaction coordinates of the F^- + $(CH)_3Cl$ reaction.

Stationary point	HF/3-21+G(d)	MP2/6-311+G(d,p)	B3LYP/6-311++G(d,p)
F^- + $(CH)_3Cl$	0.0 (0.0)	0.0 (0.0)	0.0 (0.0)
Precomplex	–34.5 (–36.2)	–28.3 (–29.5)	–30.5 (–32.3)
TS(S_N2)	–12.2 (–11.7)	–3.1 (–3.7)	–15.6 (–16.3)
TS(anti)	–18.8 (–19.9)	–13.8 (–13.8)	–20.7 (–21.3)
Late complex	–50.5 (–49.1)	–42.2 (–41.1)	–50.0 (–49.1)
Cl^- + $(CH)_3F$	–39.0 (–37.9)	–29.4 (–28.5)	–38.5 (–37.6)

Note: The energies corrected by ZPEs are given in parenthesis.

Fig. 4. The optimized structures of the F^- + $(CH)_3Cl$ reaction system at the stationary points. The bond lengths are calculated at the B3LYP/6-311++G(d,p) level.

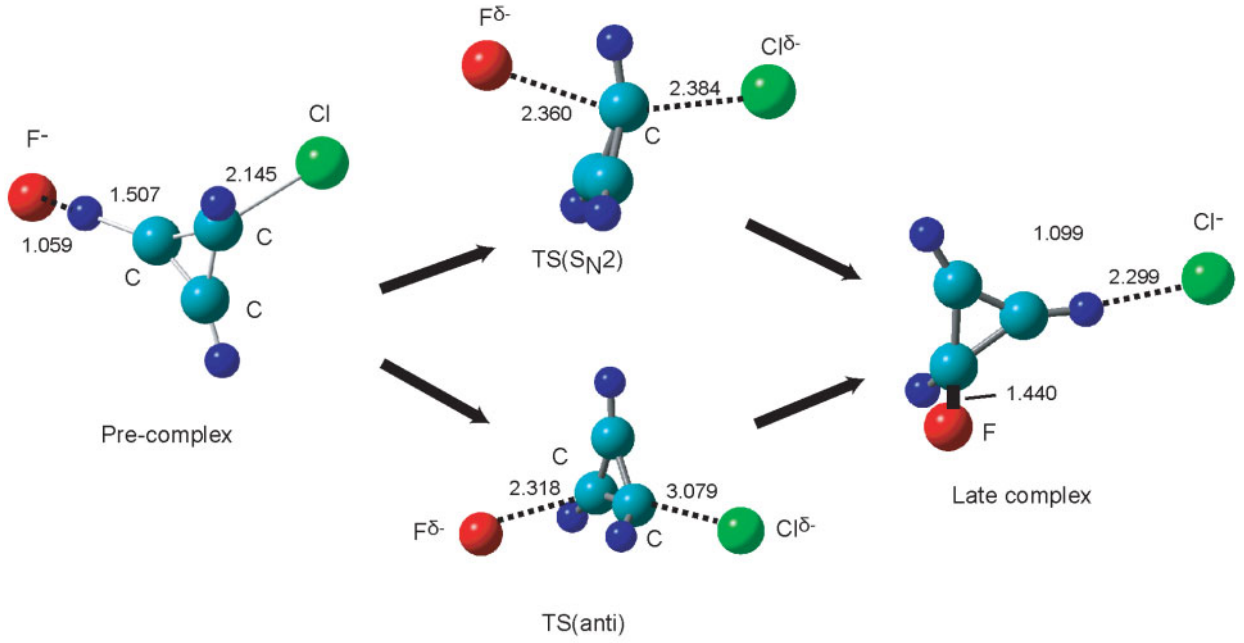

(anti) channel were calculated to be 2.318 and 3.079 Å, respectively. At the pre- and late-complexes, the halide ions bind to a hydrogen atom of $(CH)_3X$ (X = F or Cl). Details of the static properties of the reaction system, such as the geometrical structures, vibrational frequencies, and intrinsic reaction coordinate (IRC), will be discussed in a forthcoming paper.[2]

S_N2 reaction dynamics — S_N2 channel

First, a sample trajectory for the S_N2 reaction channel is discussed in this section. Snapshots of the geometrical configuration for the S_N2 reaction are given in Fig. 5. At time zero, the F^- ion is located at 8.00 Å from the center-of-mass of $(CH)_3Cl$ (R_1 = 7.342 Å). The center-of-mass collision energy is 5.0 kcal/mol. The structural parameters of $(CH)_3Cl$ were calculated as follows: the C—Cl, C1—C2, and C2=C3 bond lengths are R_2 = 1.813 Å, R_3 = 1.4876 Å, and R_4 = 1.292 Å, respectively. The highest occupied molecular orbital (HOMO) is localized in the F^- ion.

At the start of the reaction, the F^- ion gradually approaches $(CH)_3Cl$, and arrives at the precomplex region at 198 fs. The distance of F^- from the C1 atom is R_1 = 3.672 Å. The C—Cl bond is elongated from R_2 = 1.813–1.902 Å. The HOMO of the reaction system is illustrated in Fig. 5: a 2p orbital of F^- interacts slightly with the lowest unoccupied MO (LUMO) of $(CH)_3Cl$.

The trajectory passes the transition-state region at 230 fs. F^- collides the C=C double bond of $(CH)_3Cl$ at 232 fs, and the F^- distance is R_1 = 2.933 Å. The C—Cl bond length is further elongated, and the value is calculated at R_2 = 2.115 Å. The HOMO is delocalized over the complex.

At 250 fs, F^- is closer to the C1 atom. Distribution of HOMO on the Cl atom becomes larger. The geometrical parameters are R_1 = 2.761 Å and R_2 = 2.463 Å, while the C1—C2 and C2—C3 bond lengths are 1.363 and 1.331 Å, respectively, indicating that the double bond of the C2=C3 bond becomes a single bond as at 250 fs. Walden inversion of the carbon atom (C1) occurs at 260 fs and then it reaches the late complex at 300 fs. At the final stage, the products ($(CH)_3F$ and Cl^-) are formed, and Cl^- leaves rapidly from $(CH)_3F$. It was clearly found that the 2p orbital of F^- strongly interacts with C—Cl σ* orbital.

[2] H. Tachikawa. To be published.

Fig. 5. Snapshots of the conformations for the sample trajectory of the S_N2 reaction channel. The initial parameters are the distances, R_1 = 7.3424 Å, R_2 = 1.8133 Å, R_3 = 1.4876, and R_4 = 1.2915 Å. The center-of-mass collision energy (E_{coll}) is 5.0 kcal/mol. The 3-21+G(d) basis set was used for the reaction system. The time propagations for HOMO are illustrated by the iso surface.

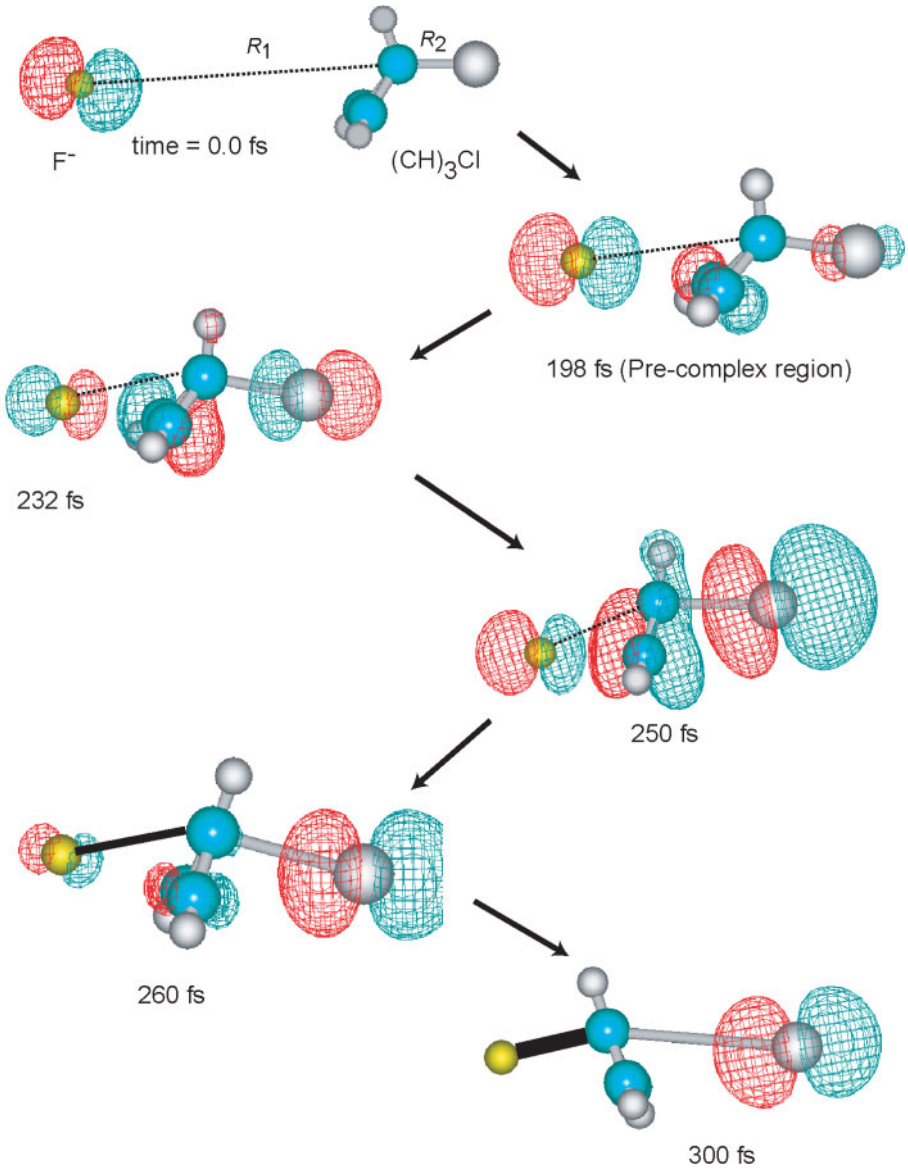

To elucidate the reaction dynamics of F^- with $(CH)_3Cl$ in more detail, time propagation of the potential energy (PE), intra- and inter-molecular distances and angles are plotted in Fig. 6. This trajectory corresponds to that given in Fig. 5. The PE of the reaction system plotted as a function of reaction time is given in Fig. 6A. Parts B and C of Fig. 6 give the intermolecular distances (R_1 and R_2) and angles (θ_1), respectively.

At time zero, F^- is located at R_1 = 7.342 Å from $(CH)_3Cl$. After starting of the reaction, PE gradually decreases as reaction time is increased, and it reaches –10.0 kcal/mol at 198 fs. This point corresponds to the precomplex region expressed by $F^-\cdots(CH)_3Cl$. The peak of PE is found at 232 fs. This peak is formed by the collision of F^- at the C=C double bond of $(CH)_3Cl$. However, the S_N2' reaction does not occur in the case of this trajectory because F^- collides at the center of the C=C bond, not at the carbon atom (C). Walden inversion and bond-forming and bond-breaking processes take place at 250–300 fs (transition-state region). The time propagation of R_1, R_2, and θ_1 around 200–300 fs shows explicit evidence of the S_N2 reaction. After the Walden inversion, the trajectory passes the late complex region (340 fs) and PE vibrates strikingly. This is due to the fact that the excess energy formed by the reaction is efficiently transferred into the C—F stretching mode of $(CH)_3F$. The translational energy of Cl^- is calculated to be 2.4 kcal/mol, which is 5.4% of the total available energy of the reaction. Almost all the energy of the reaction is transferred into the internal modes of $(CH)_3F$ in the case of this trajectory.

S_N2 reaction dynamics — S_N2' (anti) channel

A sample trajectory for the S_N2 (anti) reaction channel is

Fig. 6. Results of the sample trajectory for the S_N2 reaction channel. (A) Potential energy of the system, (B) inter- and intra-atomic distances (R_1 and R_2), and (C) angles vs. reaction time. The initial condition for the trajectory calculation is the same as that in Fig. 5.

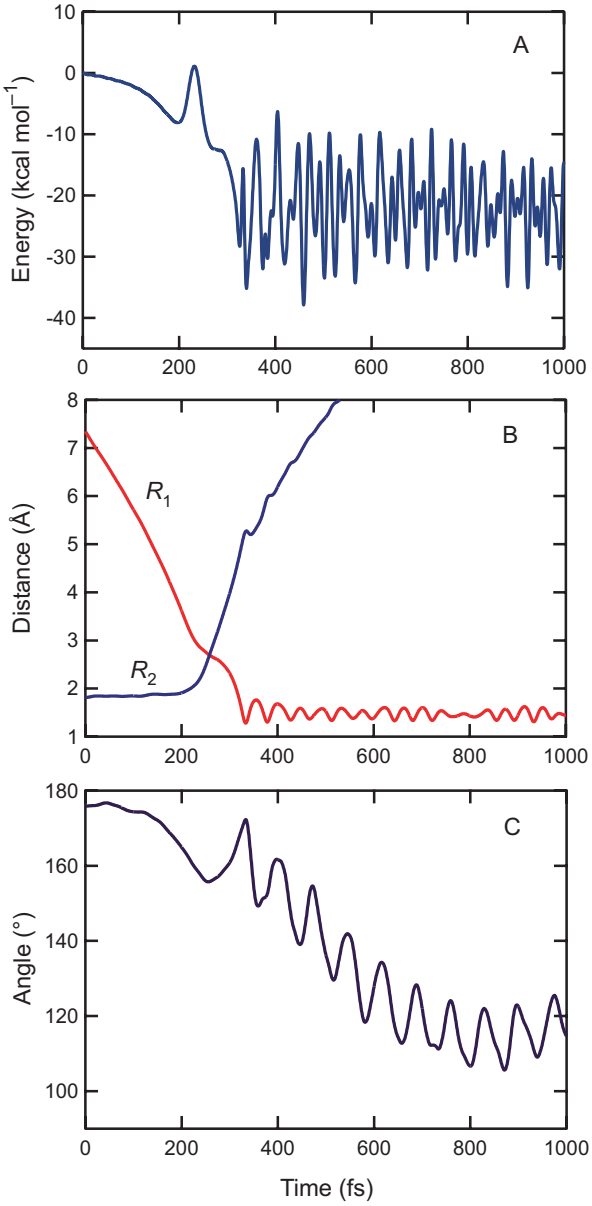

discussed in this section. Snapshots of the geometrical configuration for the S_N2 (anti) reaction are given in Fig. 7. The F^- ion is located at R_1 = 6.228 Å at time zero. The center-of-mass collision energy is 5.0 kcal/mol. The HOMO is composed of a 2p orbital of the F^- ion.

At 140 fs, the distance of F^- from the C2 atom is R_1 = 3.626 Å and the C—Cl bond length is 1.895 Å. After that, the trajectory arrives at the precomplex region at 175 fs (R_1 = 2.659 Å and R_2 = 1.9273 Å). At 200 fs, the trajectory reaches the transition-state region. The HOMO of the system is composed of the C—F σ* orbital (LUMO) of $(CH)_3Cl$ and the HOMO of F^-. The F^- distance is R_1 = 1.522 Å at 235 fs, where the trajectory passes the late complex region. The C—Cl bond is largely elongated (R_2 = 2.934 Å).

From the present results, it is explicitly found that the bond forming of C—F and the bond breaking of C—Cl take place as a result of the approaching of F^- to $(CH)_3Cl$. The 2p orbital of F^- gradually interacts with the orbital of $(CH)_3Cl$. As a result of the collision of the F^- ion at the C2 atom of $(CH)_3Cl$, the Cl^- ion is dissociated from the $(CH)_3Cl$: namely, the S_N2' (anti) reaction takes place.

Time propagations of the potential energy, intra- and inter-molecular distances and angles are plotted in Fig. 8. At time zero, F^- is 8.0 Å from $(CH)_3Cl$. After the reaction has started, PE gradually decreases as reaction time is increased, and it reaches –10.0 kcal/mol at 190 fs. During this process, the R_1 distance linearly deceases as a function of reaction time, and the energy of the system decreases. This means that the approach of F^- to $(CH)_3Cl$ causes an energy lowering because of the attractive ion–dipole interaction. At 190 fs, PE reaches a minimum corresponding to the precomplex expressed by $F^-\cdots(CH)_3Cl$. The lifetime of the complex is very short (τ < 30 fs), and the trajectory rapidly reaches the TS. After TS, PE suddenly decreases to –38.0 kcal/mol at 220 fs. This point is located in the late-complex region. PE rapidly vibrates with an amplitude of ca.10 kcal/mol after the reaction. The relative translational energy between Cl^- and $(CH)_3F$ was calculated to be 8.4 kcal/mol, which is ca. 20% of the total available energy of the reaction.

The time propagations of the C—C bond lengths (R_3, R_4, and R_5) are plotted in Fig. 8C. Before reaction, the bond lengths are R_3 = R_5 = 1.487 Å and R_4 = 1.292 Å, indicating that R_4 is the C=C double bond at time zero. The C2—C3 bond is drastically changed from 1.292 to 1.50 Å around 200 fs. Also, at the same time, R_5 (= C1—C3) is suddenly changed from 1.478 to 1.300 Å. This indicates that the exchanges of single and double bonds are occurred in the transition-state region.

Discussion

Summary

In the present study, direct ab initio MD calculations were carried out for rxn. [1] using the 3-21+G(d) basis set. Two reaction channels were examined: namely, S_N2 and S_N2' (anti) channels. The dynamics calculations showed that both reaction channels mainly occur by direct mechanism: namely, the trajectory quickly passes through the TS and the complex regions (pre- and late-complex regions). This is due to the fact that the reaction energy is significantly large (about 38 kcal/mol) and also, the basins of the complex regions are shallow for the product channel. Therefore, almost all trajectories proceed via direct mechanism.

The reaction channel is strongly dependent on the collision site of F^- around the $(CH)_3Cl$ molecule. Almost all trajectories lead to the S_N2' reaction channel, while specific collision gives the S_N2 reaction channel. This result originates from the lower activation barrier of the S_N2' (anti) channel. The branching ratios of reaction channels are roughly estimated from the results of the trajectory calculation: they are 0.2 for S_N2 and 0.8 for S_N2' (anti). However, the ratios were obtained from only 40 trajectories. To eluci-

Fig. 7. Snapshots of the conformations for the sample trajectory of the S_N2' (anti) reaction channel. The initial parameters are the distances, R_1 = 6.228 Å, R_2 = 1.815 Å, R_3 = 1.482, and R_4 = 1.291 Å. The center-of-mass collision energy (E_{coll}) is 5.0 kcal/mol. The 3-21+G(d) basis set was used for the reaction system. The time propagations for HOMO are illustrated by the iso surface.

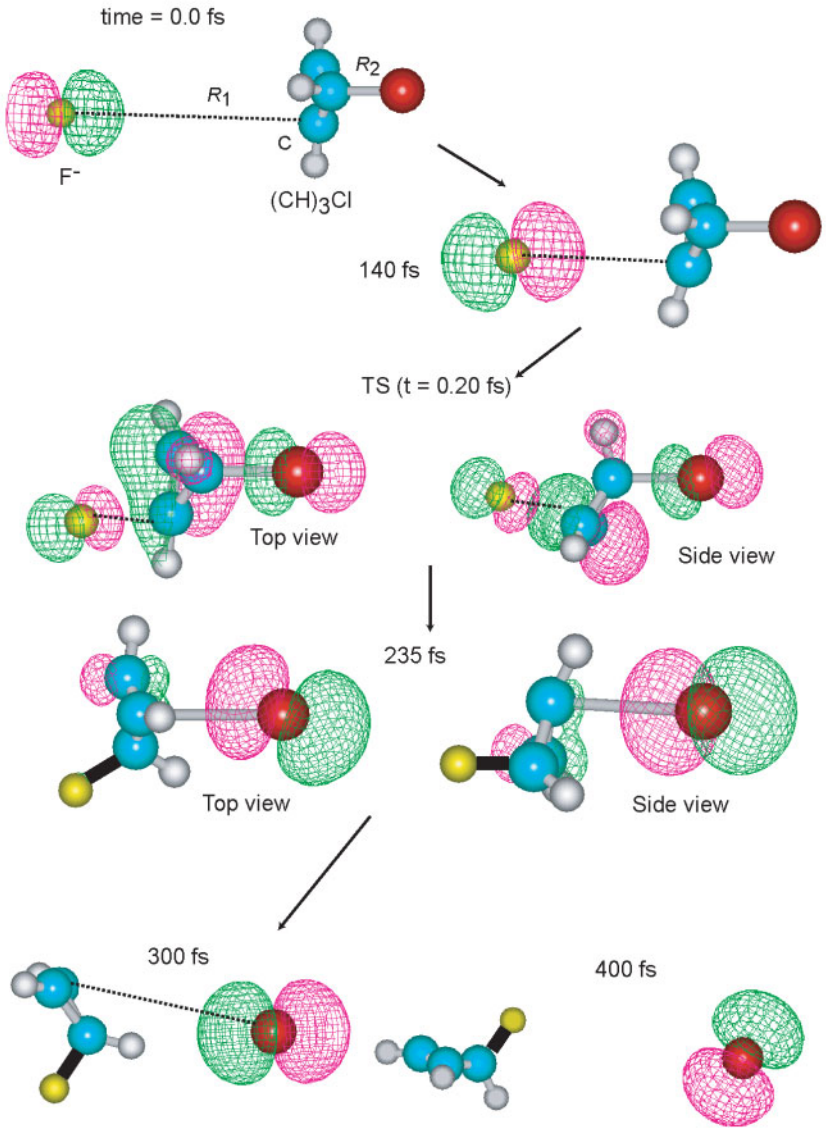

date more accurate values, a larger number of trajectories will be required.[2]

In the present study, S_N2 and S_N2' (anti) channels were examined in low-collision energy (E_{coll} = 5 kcal/mol); whereas the S_N2' (syn) channel was not considered. This is due to the fact that the S_N2' (syn) channel has a high activation barrier and needs higher collision energy. In the forthcoming work, we will calculate the S_N2' (syn) channel.[2]

Comparison with previous studies

Recently, a PE diagram for the similar S_N2 reaction (rxn. [2]) was calculated by Kim et al. (11). Their calculations indicated that the energy level of the transition state for rxn. [2] is lower than that of the initial separation, which is in good agreement with the present calculation. The reaction they used is the symmetric system (X = Y), which is slightly different from the present system. However, the structures at the stationary points are very similar to those of the present calculations.

Concluding remarks

We have introduced several approximations to calculate the PES and to treat the reaction dynamics. First, we assumed a HF/3-21+G(d) multidimensional PES in the trajectory calculations throughout. As shown in the Results and discussion, the energy profile calculated at the HF/3-21+G(d) level is in good agreement with that of the B3LYP/6-311++G(d,p) level, and it reasonably reproduces the PES. Therefore, it is enough to discuss at least qualitatively the reaction dynamics for the F^- + $(CH)_3Cl$ reaction system. However, more accurate wave functions and accurate methods may provide a deeper insight into the dynamics.

Fig. 8. Results of the sample trajectory for the S_N2' (anti) channel. (A) Potential energy of the system, (B) inter- and intra-atomic distances (R_1 and R_2), and (C) C—C bond lengths (R_3, R_4, and R_5) vs. reaction time. The initial condition of the trajectory calculation is the same as that in Fig. 7.

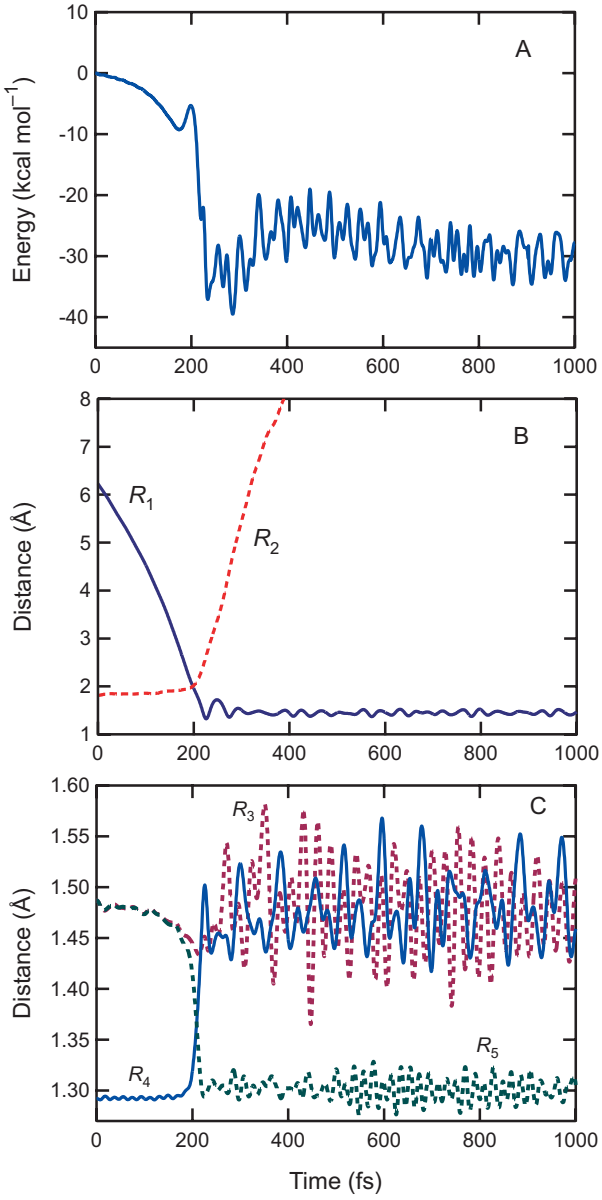

Second, we calculated only 40 trajectories for constant collision energy (E_{coll} = 5.0 kcal/mol). The number of trajectories in the present work may be enough to discuss the at least qualitative feature of the dynamics. However, larger number of trajectories in wide range of collision energies would give a more detailed reaction mechanism. Despite several assumptions introduced here, the results enable us to obtain valuable information on the mechanism of the S_N2 and S_N2' (anti) reactions. The trajectory calculations for the random collisions are now in progress.[2]

Acknowledgments

The author is indebted to the Computer Center at the Institute for Molecular Science (IMS) for the use of the computing facilities. The author also acknowledges partial support from a Grant-in-Aid for Scientific Research (C) from the Japan Society for the Promotion of Science (JSPS).

References

1. For a selection of experimental works on the gas-phase S_N2 reaction, see: (*a*) W.N. Olmstead and J.I. Brauman. J. Am. Chem. Soc. **99**, 4219 (1997); (*b*) T. Su, R.A. Morris, A.A. Viggiano, and J.F. Paulson. J. Phys. Chem. **94**, 8426 (1990); (*c*) A.A. Viggiano, J.S. Paschkewitz, R.A. Morris, J.F. Paulson, A. Gonzalez-Lafont, and D.G. Truhlar. J. Am. Chem. Soc. **113**, 9404 (1991); (*d*) C.H. DePuy, S. Gronert, A. Mullin, and V.M. Bierbaum. J. Am. Chem. Soc. **112**, 8650 (1990); (*e*) S. Gronert, C.H. DePuy, and V.M. Bierbaum. J. Am. Chem. Soc. **113**, 4009 (1991); (*f*) S.T. Graul and M.T. Bowers. J. Am. Chem. Soc. **113**, 9696 (1991); (*g*) S.T. Graul and M.T. Bowers. J. Am. Chem. Soc. **116**, 3875 (1994); (*h*) S.L. Van Orden, R.M. Pope, and S.W. Buckner. Org. Mass Spectrom. **26**, 1003 (1991); (*i*) D.M. Cyr, L.A. Posey, G.A. Bishea, C.-C. Han, and M.A. Johnson. J. Am. Chem. Soc. **113**, 9697 (1991); (*j*) D.M. Cyr, G.A. Bishea, M.G. Scarton, and M.A. Johnson. J. Chem. Phys. **97**, 5911 (1992); (*k*) K. Giles and E.P. Grimsrud. J. Phys. Chem. **96**, 6680 (1992); (*l*) W.B. Knighton, J.A. Boghar, P.M. O'Connor, and E.P. Grimsrud. J. Am. Chem. Soc. **115**, 12079 (1993); (*m*) K.E. Sahlstrom, W.B. Knighton, and E.P. Grimsrud. J. Phys. Chem. A, **101**, 1501 (1997); (*n*) A.A. Viggiano, R.A. Morris, J.S. Paschkewitz, and J.F. Paulson. J. Am. Chem. Soc. **114**, 10477 (1992); (*o*) B.D. Wladkowski, K.F. Lim, W.D. Allen, and J.I. Brauman. J. Am. Chem. Soc. **114**, 9136 (1992); (*p*) A.A. Viggiano, R.A. Morris, T. Su, B.D. Wladkowski, S.L. Craig, M. Zhong, J.I. Brauman. J. Am. Chem. Soc. **116**, 2213 (1994); (*q*) S.L. Craig and J.I. Brauman. Science (Washington, D.C.), **276**, 1536 (1997); (*r*) A.A. Viggiano and R.A. Morris. J. Phys. Chem. **98**, 3740 (1994); (*s*) C. Li, P. Ross, J.E. Szulejko, and T.B. McMahon. J. Am. Chem. Soc. **118**, 9360 (1996); (*t*) S.L. Craig and J.I. Brauman. J. Phys. Chem. A, **101**, 4745 (1997); (*u*) V.F. DeTuri, P.A. Hintz, and K.M. Ervin. J. Phys. Chem. A, **101**, 5969 (1997); (*v*) J.V. Seeley, R.A. Morris, A.A. Viggiano, H. Wang, and W.L. Hase. J. Am. Chem. Soc. **119**, 577 (1997); (*w*) J.-L. Le Garrec, B.R. Rowe, J.L. Queffelec, J.B.A. Mitchell, and D.C. Clary. J. Chem. Phys. **107**, 1021 (1997); (*x*) M.L. Chabinyc, S.L. Craig, C.K. Regan, and J.I. Brauman. Science (Washington, D.C.), **279**, 1882 (1998); (*y*) P.M. Hierl, J.F. Paulson, and M.J. Henchman. J. Phys. Chem. **99**, 15655 (1995).
2. For a selection of theoretical studies of S_N2 reactions, see: (*a*) V.M. Ryaboy. *In* Advances in classical trajectory methods. Vol. 2. *Edited by* W.L. Hase. JAI Press, Greenwich, Connecticut. 1994. pp. 115–145; (*b*) S.R. Vande Linde and W.L. Hase. J. Phys. Chem. **94**, 2778 (1990); (*c*) S.C. Tucker and D.G. Truhlar. J. Am. Chem. Soc. **112**, 3338 (1990); (*d*) G.D. Billing. Chem. Phys. **159**, 109 (1992); (*e*) B.D. Wladkowski, W.D. Allen, and J.I. Brauman. J. Phys. Chem. **98**, 13532 (1994); (*f*) H. Wang, L. Zhu, and W.L. Hase. J. Phys. Chem. **98**, 1608 (1994); (*g*) H. Wang and W.L. Hase. J. Am. Chem. Soc. **117**, 9347 (1995); (*h*) W.-P. Hu and D.G. Truhlar. J. Am. Chem. Soc. **117**, 10726 (1995); (*i*) M.N. Glukhovtsev, A. Pross, and L. Radom. J. Am. Chem. Soc. **117**, 2024 (1995); (*j*) M.N. Glukhovtsev, A. Pross, and L. Radom. J. Am. Chem. Soc. **118**, 6273 (1996); (*k*) H. Wang and W.L. Hase. Chem. Phys. **212**,

247 (1996); (*l*) D.C. Clary and J. Palma. J. Chem. Phys. **106**, 575 (1996); (*m*) H. Wang, E.M. Goldfield, and W.L. Hase. J. Chem. Soc. Faraday Trans. **93**, 737 (1997); (*n*) P. Botschwina, M. Horn, S. Seeger, and R. Oswald. Ber. Bunsen–Ges. **101**, 387 (1997); (*o*) T. Baer and W.L. Hase. *In* Unimolecular reaction dynamics — Theory and experiments. Oxford University Press, New York. 1996.

3. For trajectory studies for the S_N2 reaction, see: (*a*) S.R. Vande Linde and W.L. Hase. J. Phys. Chem. **94**, 6148 (1990); (*b*) S.R. Vande Linde and W.L. Hase. J. Chem. Phys. **93**, 7962 (1990); (*c*) G.H. Peslherbe, H. Wang, and W.L. Hase. J. Chem. Phys. **102**, 5626 (1995); (*d*) Y.J. Cho, S.R. Vande Linde, L. Zhu, and W.L. Hase. J. Chem. Phys. **96**, 8275 (1992); (*e*) W.L. Hase and Y.J. Cho. J. Chem. Phys. **98**, 8626 (1993); (*f*) H. Wang, G.H. Peslherbe, and W.L. Hase. J. Am. Chem. Soc. **116**, 9644 (1994); (*g*) G.H. Peslherbe, H. Wang, and W.L. Hase. J. Am. Chem. Soc. **118**, 2257 (1996); (*h*) W.L. Hase. Science (Washington, D.C.), **266**, 998 (1994); (*i*) H. Wang and W.L. Hase. Int. J. Mass Spectrom. Ion Process. **167**, 573 (1997); (*j*) G. Li and W.L. Hase. J. Am. Chem. Soc. **121**, 7124 (1999); (*k*) H. Wang and W.L. Hase. J. Am. Chem. Soc. **199**, 3093 (1997); (*l*) S.L. Craig and J.I. Brauman. J. Phys. Chem. A, **101**, 4745 (1997); (*m*) L. Sun, W.L. Hase, and K. Song. J. Am. Chem. Soc. **123**, 5753 (2001).
4. For a selection of quantum-scattering studies for the S_N2 reaction, see: (*a*) D.C. Clary and J. Palma. J. Chem. Phys. **106**, 575 (1997); (*b*) S. Schmatz and D.C. Clary. J. Chem. Phys. **110**, 9483 (1999); (*c*) M.I. Hernandez, J. Campos-Martinez, P. Villarreal, S. Schmatz, and D.C. Clary. Phys. Chem. Chem. Phys. **1**, 1197 (1999).
5. H. Tachikawa. J. Phys. Chem. A, **105**, 1260 (2001).
6. H. Tachikawa. J. Phys. Chem. A, **104**, 497 (2000).
7. H. Tachikawa and M. Igarashi. Chem. Phys. Lett. **303**, 81 (1999).
8. M. Igarashi and H. Tachikawa. Int. J. Mass Spectrom. **181**, 151 (1998).
9. H. Tachikawa, M. Igarashi, and T. Ishibashi. Chem. Phys. Lett. **363**, 355 (2002).
10. H. Tachikawa, M. Igarashi, and T. Ishibashi. J. Phys. Chem. A, **106**, 10977 (2002).
11. C.K. Kim, H.G. Li, B.-S. Lee, C.K. Kim, H.W. Lee, and I. Lee. J. Org. Chem. **67**, 1953 (2002).
12. H. Tachikawa. Chem. Phys. Lett. **370**, 188 (2003).
13. H. Tachikawa and H. Kawabata. J. Phys. Chem. B, **107**, 1113 (2003).
14. H. Tachikawa, M. Igarashi, and T. Ishibashi. J. Phys. Chem. A, **107**, 7505 (2003).
15. H. Tachikawa. J. Phys. Chem. A, **108**, 7853 (2004).
16. M.J. Frisch, G.W. Trucks, H.B. Schlegel, G.E. Scuseria, M.A. Robb, J.R. Cheeseman, J.A. Montgomery, Jr., T. Vreven, K.N. Kudin, J.C. Burant, J.M. Millam, S.S. Iyengar, J. Tomasi, V. Barone, B. Mennucci, M. Cossi, G. Scalmani, N. Rega, G.A. Petersson, H. Nakatsuji, M. Hada, M. Ehara, K. Toyota, R. Fukuda, J. Hasegawa, M. Ishida, T. Nakajima, Y. Honda, O. Kitao, H. Nakai, M. Klene, X. Li, J.E. Knox, H.P. Hratchian, J.B. Cross, C. Adamo, J. Jaramillo, R. Gomperts, R.E. Stratmann, O. Yazyev, A.J. Austin, R. Cammi, C. Pomelli, J.W. Ochterski, P.Y. Ayala, K. Morokuma, G.A. Voth, P. Salvador, J.J. Dannenberg, V.G. Zakrzewski, S. Dapprich, A.D. Daniels, M.C. Strain, O. Farkas, D.K. Malick, A.D. Rabuck, K. Raghavachari, J.B. Foresman, J.V. Ortiz, Q. Cui, A.G. Baboul, S. Clifford, J. Cioslowski, B.B. Stefanov, G. Liu, A. Liashenko, P. Piskorz, I. Komaromi, R.L. Martin, D.J. Fox, T. Keith, M.A. Al-Laham, C.Y. Peng, A. Nanayakkara, M. Challacombe, P.M.W. Gill, B. Johnson, W. Chen, M.W. Wong, C. Gonzalez, and J.A. Pople. GAUSSIAN 03. Revision B.04 [computer program]. Gaussian, Inc., Pittsburgh, Penn. 2003.